OXIDE POWDERS FROM TARTARIC ACID Mg/Zr COORDINATION COMPOUNDS WITH CO_2 ADSORPTION PROPERTIES
PULBERI OXIDICE OBŢINUTE DIN COMPUŞII COORDINATIVI AI ACIDULUI TARTARIC CU Mg/Zr CU PROPRIETĂŢI ADSORBANTE PENTRU CO_2

LIGIA TODAN *, DANIELA C. CULIȚĂ, DOREL CRIŞAN, NICOLAE DRĂGAN, JEANINA PANDELE-CUŞU, FLORICA PAPA

"Ilie Murgulescu" Institute of Physical Chemistry, Romanian Academy, 202 Splaiul Independentei, 060021 Bucharest, Romania

Mono- and bicomponent coordination compounds of Mg-Zr with tartaric acid were synthesized in an aqueous solution, at two different Mg/Zr molar ratios. Part of the obtained amorphous precursors were thermally treated at 650^{0}C, the other part was calcined at 1000^{0}C, forming thus MgO-ZrO_2 powders. The structure and properties of the precursors and of the oxide powders were determined by thermal analysis, FTIR, XRD, BET method for surface area and pore volume, CO_2 adsorption. The influence of the thermal treatment temperature on the powders characteristics was considered. The coordination modes of the tartaric carboxilic groups in Mg, respectively or/and Zr-containing precursors is dissimilar and the dehydration and crystallization processes in the binary powders differ too. High-temperature ZrO_2 polymorphs stabilized at low temperature by including the Mg^{2+} in the lattice, decrease in content with the raise of temperature, partialy turning into monoclinic zirconia.The specific surface area and porosity as well as the CO_2 adsorption properties of the samples treated at 650^{0}C are significantly higher than the ones of the powders calcined at 1000^{0}C. The CO_2 adsoption efficiency of the binary oxides is lower than the one of MgO but higher when compared to ZrO_2, one of the samples showing the best performance, although the Mg/Zr molar ratio in the binary calcined oxides is about the same. The oxide powders were stable at recycling.

Compuşi coordinativi mono- şi bicomponenţi ai Mg-Zr cu acidul tartric, au fost sintetizaţi în soluţie apoasă, la două rapoarte molare diferite Mg/Zr. O parte din precursorii amorfi obţinuţi a fost tratată termic la 650^{0}C, cealaltă parte a fost calcinată la 1000^{0}C, formând astfel pulberi MgO-ZrO_2. S-au determinat structura şi proprietăţile precursorilor şi a pulberilor oxidice prin analiză termică, FTIR, XRD, metoda BET pentru aria suprafeţei şi volumul porilor, adsorpţia de CO_2. A fost examinată influenţa temperaturii de tratament termic asupra caracteristicilor pulberilor. Modurile de coordinaţie ale grupărilor carboxilice ale acidului tartric în precursorii conţinând Mg, respectiv sau/şi Zr sunt diferite şi procesele de deshidratare şi cristalizare ale pulberilor binare diferă de asemenea. Conţinutul formelor polimorfe de temperatură înaltă ale ZrO_2 care sunt stabilizate la temperatură joasă prin includerea Mg^{2+} în reţea, scade cu creşterea temperaturii, transformându-se parţial în zirconie monoclinică. Aria specifică a suprafeţei şi porozitatea ca şi capacitatea de adsorpţie a CO_2 ale probelor tratate la 650^{0}C sunt semnificativ mai mari decât cele ale pulberilor calcinate la 1000^{0}C. Oxizii binari au o eficienţă de adsorpţie a CO_2 mai scăzută decât cea a MgO, dar mai ridicată decât cea a ZrO_2, una dintre probe având cea mai bună performanţă, deşi oxizii binari calcinaţi au cam acelaşi raport molar Mg/Zr. Pulberile oxidice au fost stabile la reciclare.

Keywords: *MgO-ZrO_2 oxide powders, tartaric acid complexes, solution-gel, thermal analysis, CO_2 adsorption*

1. Introduction

CO_2 is an air pollutant generated from combustion processes and the control of CO_2 emission through the development of efficient technologies seems to be an important task. There are several methods for CO_2 capture and among them the adsorption on solid adsorbents has become of interest due to some advantages such as low operation costs, greater convenience, energy-efficiency [1].

Due to the wide range of operating conditions in the CO_2 capture technologies, a variety of specific adsorbents is used for each application. Due to the acidic nature of CO_2 molecule, the presence of basicity sites like the ones in alkaline oxides can enhance CO_2 adsorption capacity. Transition metal species can improve the adsorptive properties of alkaline oxides lowering the regeneration energies of the metal carbonates which were formed [1].

Magnesium oxides are CO_2 sorbent candidates with moderate CO_2 sorption capacity. They perform well in a wide temperature range from room temperature to around 500^{0}C. Their advantages are a wide availability in natural minerals at low costs. Modified alkaline oxides-based sorbents are promoted with different elements to improve their regeneration process [2]. For instance, zirconia, a high Tammann temperature material, has been used to stabilize CaO-based sorbents. The material was obtained by

* Autor corespondent/*Corresponding author*,
E-mail: l_todan@yahoo.co.uk

a sol-gel technique and the influence of the synthesis parameters on the morphology and CO_2 uptake of the material were evaluated [3].

Different methods and precursors have been used to prepare sorbents with improved properties. Up to now a number of studies have reported the production of CaO sorbents from organometallic precursors and the relation between the structural characteristic of the alkaline oxides and their performance. The decomposition of organometallic compounds can generate meso- and macroporous structures with large surface area resulting in an enhancement of CO_2 capture [4].

The MgO-ZrO_2 system, especially nano-sized, is one of the most important categories of nanocomposites due to their chemical and thermal stability and many synthetic approaches have been developed to obtain nanopowders in the MgO-ZrO_2 mono and bicomponent system exploiting the techniques of diverse physical and/or chemical routes [5-11].

Nanocrystalline magnesia-stabilized zirconia powders have been synthesized using Pechini sol-gel process [6] or they were obtained from a citrate gel precursor by heating treatment [5]. Several other methods generated mixed magnesium-zirconium oxides with different properties, such as a peroxo-complex-mediated route [7], an evaporation-induced self-assembly method [8, 9]. MgO-ZrO_2 nanopowders and coatings were prepared by a sol-gel method using sucrose as both chelating and gel agents [10].

ZrO_2-MgO powders in a wide range of concentrations were prepared by coprecipitation of the corresponding nitrate salts and the influence of Mg^{+2} on the structure, properties and thermal behavior of the system was studied [11].

Considering the fact that magnesium oxide CO_2 sorbents as such and promoted with different elements (Al_2O_3, SiO_2, ZrO_2, etc) is a less explored domain, the aim of the present work is to obtain zirconia-magnesia composite powders using tartrate-based precursors. The effect of varying amounts of zirconia on magnesia properties and the influence of the calcination temperature on the structure and properties of the oxide powders were studied.

2. Experimental

2.1. Materials and sample preparation

All the chemical reagents were of analytical grade purity and used as received without further purification.

Tartrate-based precursors of the oxide powders, were obtained from solutions of $ZrOCl_2 \cdot 8H_2O$, $Mg(NO_3)_2 \cdot 6H_2O$ and tartaric acid. $Mg(NO_3)_2 \cdot 6H_2O$ and $ZrOCl_2 \cdot 8H_2O$ were each dissolved in a minimum amount of water. A tartaric acid solution was slowly added to the salts solutions under constant stirring and heating at 60°C. Opalescence was noticed.

In case of the binary compounds the two inorganic salt solutions were mixed before adding the tartaric acid at two Mg/Zr molar ratios, 1/1 (Mg-Zr-tart (1)) and 2/1 (Mg-Zr-tart (2)). The molar ratio metal, respectively metals/ tartaric acid was 1/1 and the one Mg/ tartaric acid was 1/2 and respectively 2/3.

The pH of the prepared solutions was about 1. The beakers containing the solutions were incubated overnight in an oven at 60°C. To improve the coordination capacity of tartaric acid, the carboxylic acid groups were deprotonated by increasing the pH to about 8-9 using NH_3 (25% aq). The resultant gel-like precipitates were kept at room temperature for about 2 h then they were filtered and repeatedly washed with hot and room temperature deionized water to clear away Cl^- and NO_3^-. Then they were dried at 100°C in an oven.

To generate oxides in mono and bicomponent systems, part of the obtained powders, the tartaric amorphous precursors, were thermally treated at 650^0C with a 6 h plateau and at a heating rate of 1^0C min^{-1} in accordance with the thermal analysis and the other part at 1000°C with a 2h plateau to test the influence of the temperature on the structure and properties of the products.

2.2. Characterization techniques

All four samples have been characterized using the following methods:

Thermal analysis up to 1000°C, using a Mettler Toledo Star System TGA/SDTA851/LF 1600°C, with a heating rate of 10^0C min^{-1}, under air atmosphere, and with a debit of 50 mL min^{-1}.

FT-IR spectroscopic measurements were performed with a FT-IR NICOLET 6700 (400-4000 cm^{-1}) spectrophotometer using thin transparent KBr pellets containing approximately 0.5% wt sample.

Powder X-ray diffraction patterns were recorded on a Rigaku's Ultima IV apparatus, with Cu Kα radiation (λ -1.54 Å), in the 2 θ = 10-70° range, operating at 40 kV and 30 mA, 0.02° step size and 5°/min scan speed. Phase identification were performed using Rigaku's PDXL software, with Whole Pattern Fitting (WPF) module, connected to ICDD PDF-2 database. A computerized analysis of the XRD spectra with a proper X-RAY5.0 program that represents the upgrade from the previous X-RAY3.0 program was accomplished.

Elemental analysis of the binary inorganic oxide samples was carried out using a wavelength dispersive X-ray fluorescence (WDXRF) spectroscopy method. The Rigaku ZSX Primus II spectrometer is equipped with an X-ray tube with Rh anode, 4.0 kW power, with front Be window, thickness: 30 microns. The measurements were performed onto pressed

pellets of 10 mm diameters under vacuum. The XRF data were analyzed using EZ-scan combined with Rigaku's SQX fundamental parameters software (standard less) which is capable of automatically correcting for all matrix effects, including line overlaps.

The specific surface area of the thermally treated powders has been determined by the Brunauer, Emmett, Teller (BET) method, using a Micromeritics ASAP 2020 apparatus. The sample has been degassed at 300°C for 2 h before analysis.

The adsorption properties for CO_2 were measured at room temperature with a Quanthachrome ChemBET 3000 apparatus equipped with a thermal conductivity detector (TCD). Before adsorption tests the samples have been subjected to pretreatment to helium flux at 500°C for one hour.Then samples were cooled down to room temperature and the CO_2 adsorption has been performed by injecting successive pulses of 100 µl of CO_2. The amount of CO_2 adsorbed was calculated from the area of obtained peaks.

3. Results and discussion

3.1.Thermal analysis of the tartrate complex compounds

The thermograms of the obtained tartaric-metal compounds are presented in Fig. 1 (a-d). Except for Mg-tart, their thermal behaviour is a multi-step process. In all cases it is completed at about 650^{0}C. At about 400^{0}C, Mg-tart sample shows a drastic mass loss accompanied by a sharp exothermic peak at 439^{0}C on the DTA curve associated with the oxidation of the decomposed organic complex and crystallization of the oxide.

Due to zirconium high degree of covalency and to the strong hydrolysis tendency of $[Zr(H_2O)_4^{4+}]$, the Zr-tart precursor should be of the hydroxyl-carboxylates type [12,13] with a more complex thermal behaviour than the previously presented one. Steps below 340^{0}C on the DTG curve correspond to the loss of weight of adsorbed and structural water and perhaps to a gradual thermal decomposition of organic groups and are accompanied by two endothermic peaks (100^{0}C and 264^{0}C). The mass loss at 563^{0}C on the TG curve should be caused by the decomposition of the organic ligand leading to crystallized compounds. This process is accompanied by a strong sharp exothermic peak on the DTA curve at 568^{0}C.

The thermograms of the binary systems show an endothermic effect due to removal of adsorbed and structural water up to 300^{0}C (Mg-Zr-tart (1)), respectively only of adsorbed water up to 100^{0}C(Mg-Zr-tart (2)). Above 300^{0}C, the thermogram shows in case of Mg-Zr-tart (2), a

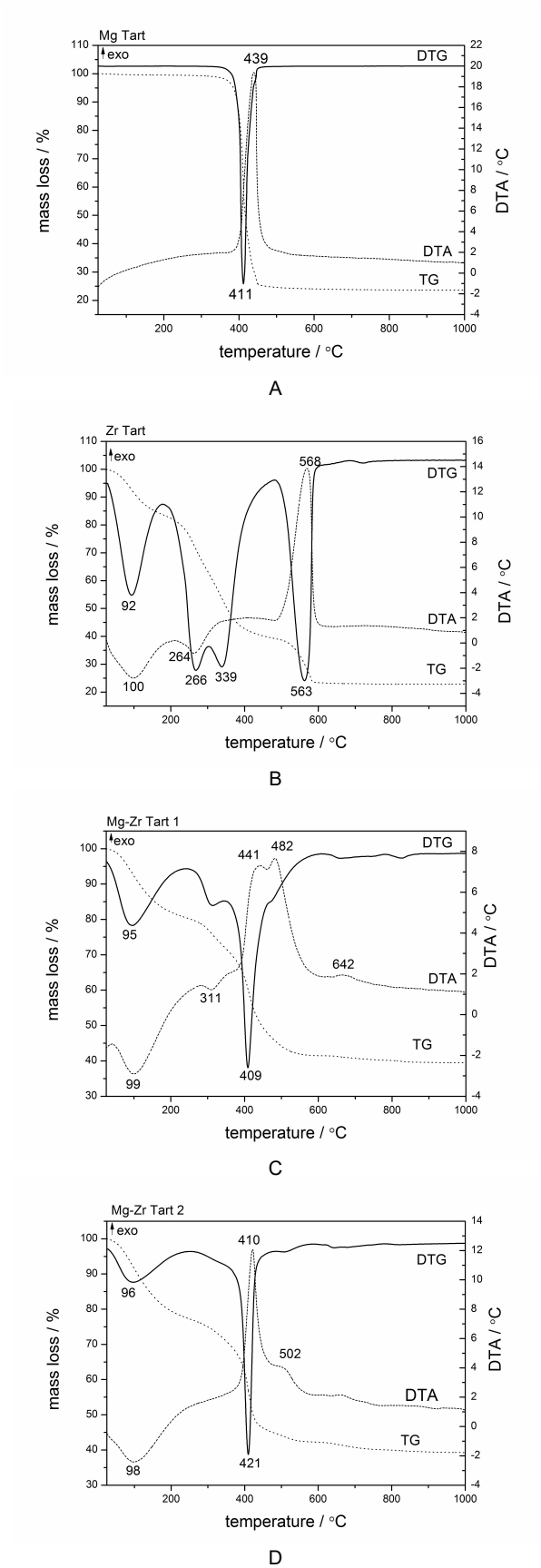

Fig. 1 - Thermal analysis of the dried gels: (a) Mg-tartrate complex; (b) Zr-tartrate complex; (c) Mg-Zr-tartrate complex (1); (d) Mg-Zr-tartrate complex (2) / *Analiza termică a gelurilor uscate: (a) complexul Mg-tartrat; (b) complexul Zr-tartrat; (c) complexul Mg-Zr-tartrat (1); (d) complexul Mg-Zr-tartrat (2)* .

sudden mass loss at 409^{0}C and respectively at 421^{0}C on the TG curve accompanied by an exothermic effect representing the decomposition of the organic complex and formation of the crystallized oxides. In case of Mg-Zr-tart (1), the mass loss at 409^{0}C generates two overlapping exothermic events (at 441^{0}C and 482^{0}C) that may indicate the formation of transient intermediate phases like oxy or dioxycarbonates before the oxide final product [14]. So there is a difference of the dehydration and crystallization processes in the binary systems (1) and (2), most likely caused by changes in the structure of the hydration shell of the amorphous gel under the influence of different Mg /tartaric acid molar ratios [15, 16]. Very small mass loss and weak exothermic processes in the 500^{0}C-650^{0}C temperature range of binary systems thermograms indicate the removal of carbonaceous residues.

3.2. *FTIR analysis of tartaric complexes*

Infrared spectroscopy was performed to examine the coordination mode of the tartrate ligand. The spectra of the mono and bicomponent tartaric complexes were recorded in the 4000 – 500 cm^{-1} range and were compared to the one of tartaric acid (Fig. 2).

As can be seen in Fig. 2, the IR spectra of the mixed oxide samples Mg-Zr-tart (1) and Mg-Zr-tart (2) are almost identical.

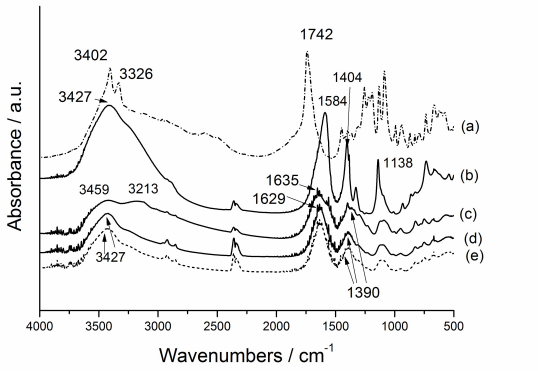

Fig. 2 - Infrared spectra of the tartaric acid (a) and of the as prepared samples: (b) Mg-tartrate complex; (c) Zr-tartrate complex; (d) Mg-Zr-tartrate (1); e) Mg-Zr-tartrate (2) / *Spectrele în infraroşu ale acidului tartric (a) şi ale probelor preparate ca atare: (b) complexul Mg-tartrat; (c) complexul Zr-tartrat*; *(d) Mg-Zr-tartrat (1); (e) complexul Mg-Zr-tartrat (2).*

A broad absorption band with a maximum around 3400 cm^{-1} in the spectra of the metal tartrate samples is due to the stretching vibrations hydroxyl groups [17]. The hydroxyl region of zirconia is broader, displaying two bands that can be assigned to surface hydroxyl groups bonded to a different number of Zr atoms [18].

The protonated tartaric acid yields an absorption band corresponding to a carbonyl stretch v(CO) at 1742 cm^{-1} and a v(C-OH) vibration at about 1200 - 1300 cm^{-1} [19-21].

The shift of these two bands to higher or lower frequencies suggests participation of COOH groups in the complex formation after deprotonation [21, 22].

In the spectra of the Mg and/or Zr samples two intense bands are noticed, characteristic for coordinated carboxylic groups, v_{asym}(OCO) (1584 cm^{-1} for Mg-tartrate, 1635 cm^{-1} for Zr-tartrate and 1629 cm^{-1} for Mg-Zr-tartrate (1) and (2)) and v_{sym}(OCO) (1404 cm^{-1} for Mg-tartrate, 1390 cm^{-1} for Zr-tartrate and Mg-Zr-tart (1) and (2)). Based on the spectroscopic criterion, the magnitude of the separation $\Delta v = v_{asym} - v_{sym}$ can be used to indicate the coordination mode of the carboxylate ions [17, 18]. In case of Mg-tartrate complex, Δv = 180 cm^{-1} is smaller than the value of the parameter of the ionic compound ($\Delta v(Na_2tart)$ = 240 cm^{-1}) [20] suggesting a bidentate coordination for the carboxylate groups of the tartrate ligand. Considering Δv for Zr-tartrate (245 cm^{-1}) and Mg-Zr-tartrate (1) and (2) (229 cm^{-1}) one can predict bridging coordination mode of the metals with the tartrate anion which may involve binding to one oxygen atom of the carbonyl group and to a water molecule, confirming thus the thermal analysis results [20, 23, 24, 25].

The band at 1138 cm^{-1} in the spectrum of the Mg-tartrate can be attributed to the C-O stretching vibration of the protonated secondary alcohol OH groups [19, 20]. This band broadens in case of Zr-tartrate and Mg-Zr-tartrate samples as well as the one at ~ 1400 cm^{-1} attributed to v_{sym}(OCO), an overlapping with Zr=O from zirconyl vibration band (in the 1070 - 1030 cm^{-1} range) in the first case and in the second one with Zr-OH bending vibration bands (1350 cm^{-1}) being possible [12, 23].

3.3. *FTIR analysis of the thermally treated oxide samples*

The infrared spectra of the powders were recorded after the thermal treatment up to 650 °C (Fig. 3). As can be noticed, no relevant bands indicating the presence of organic ligands or fragments are observed, in agreement with the pure mono and bi-component oxides. OH stretching bands can be noticed at about 3400 cm^{-1} and OH bending bands appear in the 1500-1600 cm^{-1} region [12]. The band at 1420 cm^{-1} corresponds to carbonate ion on the surface [26].

In the sample resulting from Mg-tartrate calcination, characteristic bands for MgO appear at 536 cm^{-1} and 440 cm^{-1} [27]. From Zr-tartrate precursor, ZrO_2 resulted with characteristic stretching and bending vibrations at 764 cm^{-1}, 579 cm^{-1}, 515 cm^{-1}, 433 cm^{-1} [12, 28].

In the spectra of the binary samples, MgO-ZrO_2 (1) and MgO-ZrO_2 (2), one broad band at

about 400 - 500 cm^{-1} could be the result of the overlapping of Mg-O and Zr-O vibrational modes.

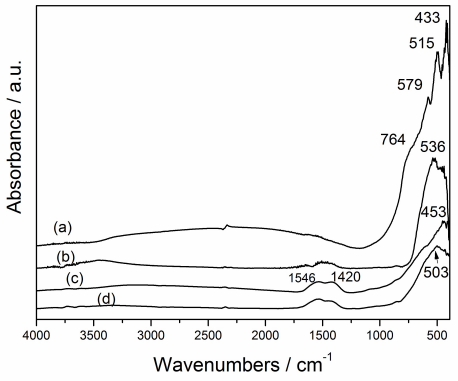

Fig. 3 - Infrared spectra of the samples thermally treated at 650^{0}C: a) ZrO_2; b) MgO; c) MgO-ZrO_2 (1); d) MgO-ZrO_2 (2) / *Spectrele în infraroşu ale probelor tratate termic la 650^{0}C: a) ZrO_2; b) MgO; c) MgO-ZrO_2 (1); d) MgO-ZrO_2 (2)* .

3.4. *X-ray diffraction of the oxides obtained by calcination of tartrate complexes*

In order to get a better insight into the structure and phase composition of the thermally treated oxides, the X-ray diffraction patterns of the powders calcined at 650^{0}C and 1000^{0}C were recorded. The diffraction patterns of the samples thermally treated at 650^{0}C are presented in Fig. 4 (a-c), and those of the samples calcined at 1000^{0}C in Figure 5 (a, b).

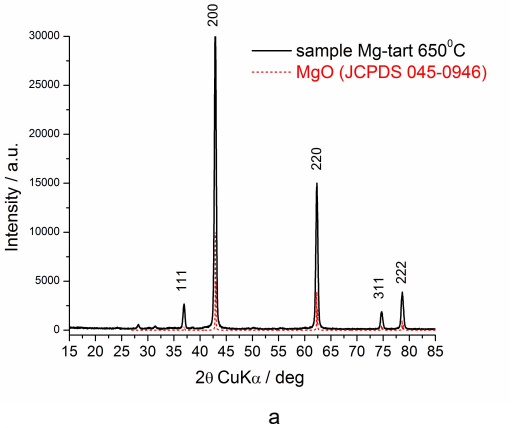

a

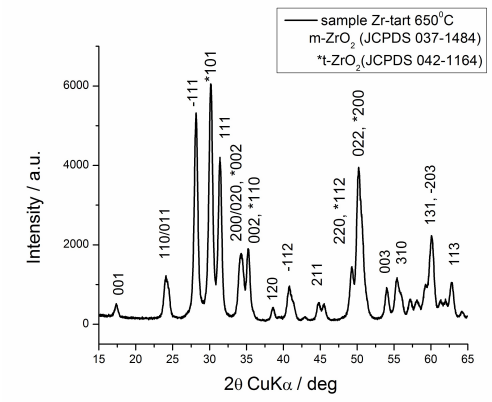

b

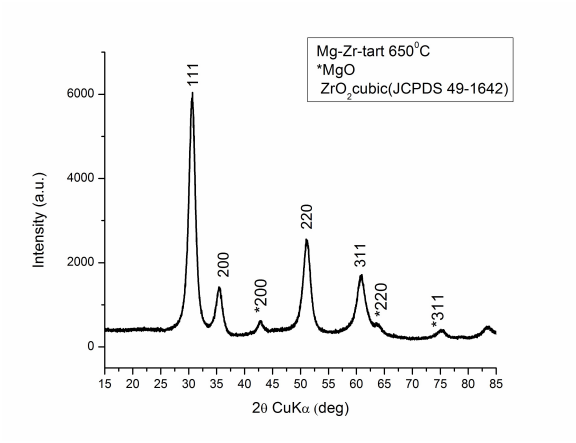

c

Fig. 4 - Diffraction pattern of the oxide powders obtained by thermal treatment at 650^{0}C of the following precursors: a) Mg-tartar; b) Zr-tartar; c) Mg-Zr-tartar / *Tiparele de difracţie ale pulberilor oxidice obţinute prin tratamentul termic la 650^{0}C al următorilor precursori: a) Mg-tartrat; b) Zr-tartrat; c) Mg-Zr-tartrat* .

The profiles of the diffraction peaks are sharp and symmetrical, suggesting well formed crystals at both temperatures. Mg-tart precursor thermally treated at 650^{0}C as well as at 1000^{0}C generated MgO periclase (JCPDS 042-1164). The diffraction patterns of monocomponent zirconia powder at 650^{0}C and 1000^{0}C showed a mixture of polymorphs, identified as monoclinic ZrO_2 (m-ZrO_2) (JCPDS 037-1484) and tetragonal ZrO_2 (t-ZrO_2) (JCPDS 042-1164). Estimating the m-ZrO_2 and t-ZrO_2 content from the relation of intensities of the reflections in the diffraction pattern [29], one could say that the increase of temperature favoured the decrease of t-ZrO_2 content. The structure of the binary (1) and (2) samples is identical at both calcinations temperatures, as shown in Fig. 5 b.

In case of the bicomponent powders, Mg^{+2} is incorporated inside ZrO_2-type lattice stabilizing thus the cubic high temperature phase [11]. Consequently by a 650^{0}C thermal treatment, Mg-Zr-tart (1) and (2) generated MgO periclase and the high temperature ZrO_2 cubic phase (fig.4-c).

As previous reports suggest [11], the phase structurally related to tetragonal or cubic zirconia is obtained after crystallization of the amorphous precursors and the temperature treatment, due to the decrease of Mg^{+2} solubility inside ZrO_2 lattice caused a transition to monoclinic zirconia [11]. In our case, the diffraction pattern of the bicomponent samples thermally treated at 1000^{0}C show beside MgO periclase the coexistence of a monoclinic and of a cubic ZrO_2.

Using the dispersive X-ray fluorescence, the proportion of the two oxides, MgO and ZrO_2, in the 1000^{0}C binary oxide samples was established. The data are presented in Table 1.

The Mg/Zr atomic ratio is approximately the same in Mg-Zr-tart (1) and Mg-Zr-tart (2), about 0.5, lower than that of the starting solution, indicating a partial loss of Mg^{2+} in the process [30].

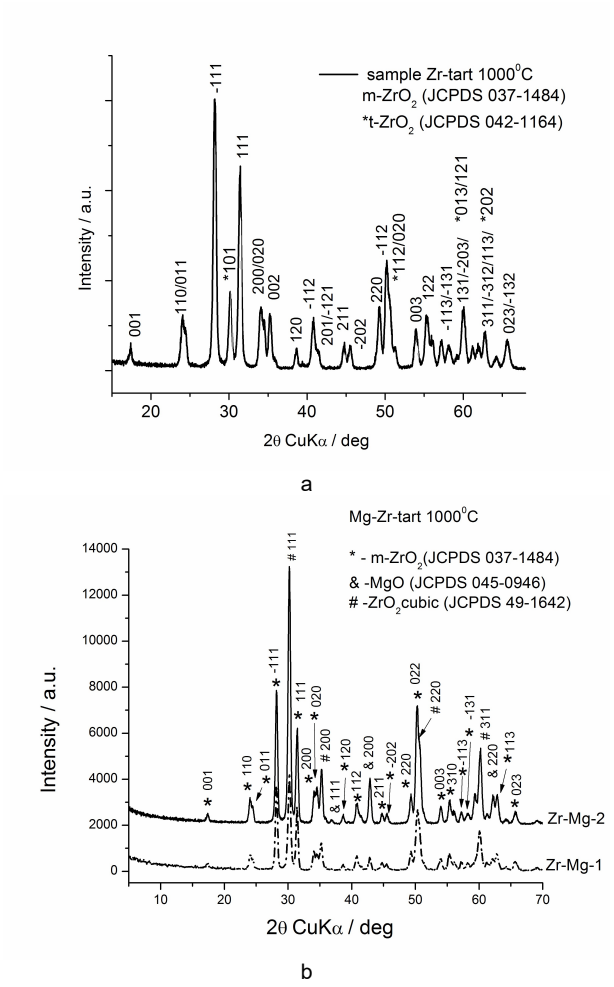

Fig. 5 - Diffraction pattern of oxide powders obtained by thermal treatment at 1000^{0}C of the following precursors: a) Zr-tartar; b) Mg-Zr-tartar (1) and (2) / *Tiparele de difracţie ale pulberilor oxidice obţinute prin tratamentul termic la 1000^{0}C al următorilor precursori: a) Zr-tartrat; b) Mg-Zr-tartrat*

Table 1

Quantitative elemental analysis of binary oxide samples by dispersive X-ray fluorescence / *Analiza elementală cantitativă prin fluorescenţă de raze X a probelor de oxizi binari*

	MgO-ZrO_2 (1) (Mass %)	**MgO-ZrO_2 (2)** (Mass %)
MgO	13.45	14.88
ZrO_2	86.55	85.12

It can be assumed that the remained quantity was bound in stable complex structures.

3.5. *Textural properties*

The textural properties of the samples thermally treated at 650^{0}C and 1000^{0}C were determined by N_2 adsoption-desorption. A higher thermal treatment temperature lowers the specific surface area and porosity of the powders. MgO sample has the largest surface area (S_{BET} = 29.53 m^2g^{-1} and respectivelly 21.9 m^2g^{-1}) followed by MgO-ZrO_2 (2) (S_{BET} = 4.4 m^2g^{-1} and respectivelly 2.9 m^2g^{-1}). MgO-ZrO_2 (1) shows a lower surface area than sample (2) at both temperatures.

3.6. *CO_2 adsorptive properties*

The obtained oxide samples, thermally treated at different temperatures, were tested for CO_2 adsorption at 50^{0}C. The results are comparativelly presented in Table 2. From the data displayed in this table, it can be observed that the adsorption properties of the group of samples treated at 650^{0}C are significantly higher than the ones of the powders calcined at 1000^{0}C. Within each group of samples the adsorption efficiency decreases in the order: MgO > MgO-ZrO_2 binary oxides > ZrO_2. While the binary samples adsorbe comparable CO_2 quantity at low temperature, at 1000^{0}C sample (1) shows a more prominent decrease of the adsorption efficiency.

Table 2

CO_2 adsorption on the samples thermally treated at different temperatures / *Adsopţia CO_2 pe probele tratate termic la diferite temperaturi*

	Thermally treated at 650^{0}C / *Tratate termic la 650^{0}C*	**Thermally treated at 1000^{0}C / *Tratate termic la 1000^{0}C***
Samples/Probe	CO_2 ads. µL/g	CO_2 ads. µL/g
MgO	905.7	596
ZrO_2	210.44	47
MgO-ZrO_2 (1)	541	145
MgO-ZrO_2 (2)	496.15	283

The CO_2 adsoptive properties can be connected with the textural properties of the samples, or with the content of high-temperature metastable ZrO_2 polymorphs, as in case of zirconia containing samples, which can generate lattice deffects [15]. An increase in the adsorption efficiency of the binary oxides compared to ZrO_2 could be attributed to the introduction of Mg^{2+} [9], not only owing to its base character but also to the oxygen vacancies generated as a result of the substitution of Zr^{+4} by Mg^{+2} in zirconia lattice which can give rise to new highly stable CO_2 adsoption configurations [31]. The fact that MgO-ZrO_2 (1) and (2) have different properties although the Mg/Zr molar ratio is about the same can be explained by the difference in the hydration shell and crystallization events of the two amorphous precursors generated in non-identical reaction medium, respectively at two different Mg/ tartaric acid ratios [16], which can generate dissimilar surface vacancies at pre-crystallization temperatures [15].

The powders were stable, could be recycled by heating at 500 °C and they maintained their activity after two adsorption/desoption cycles.

4. Conclusions

Crystalline oxide powders in the mono and binary MgO-ZrO_2 systems were obtained using coordination compounds of the metals with tartaric acid as precursors, followed by thermal treatment.

A stable complex structure was generated in which the coordination mode of carboxilate ion in Mg-tart is different from that in the Zr-tart and Mg-Zr-tart (1) and (2); in the first case the metal ion interacts equally with the two oxygen atoms of a COO^- group and in the second case the water molecule may replace one of the two ligands. Binary MgO-ZrO_2 with about the same Mg/Zr molar ratios were obtained, lower from the ones used in the synthesis.

Reacting medium and calcination temperature has an important role in determining the crystallinity, phase composition, textural and CO_2 adsorptive properties of the oxide powders.

The binary oxides show lower performances than MgO but improved properties compared to zirconia due to the presence of Mg^{+2} as such and incorporated inside ZrO_2-type lattice owing to its base character as well as to the lattice deffects which can form stable CO_2 adsoption configurations.

The binary samples have approximately the same CO_2 adsoption efficiency when obtained at lower thermal treatment temperature but when formed at higher temperature, sample (2) shows a better behavior than sample (1), despite the fact that they have about the same composition; the different initial molar ratio Mg /tartaric acid generates dissimilarities in the hydration shell and crystallization events of the amorphous precursors and thus dissimilar surface deffects at pre-crystallization temperatures appear.

Acknowledgements

The paper ,Oxide powders from tartaric acid Mg/Zr coordination compounds with CO_2 adsorption properties' has been performed in the frame of the 4.12 Project of the Romanian Academy Program 'Oxide systems obtained by chemical methods, in solution' (2017-2018) of the Ilie Murgulescu Institute.

REFERENCES

1. K. C. Chanapattharapol, S. Krachuamran, S. Youngme, Study of CO_2 adsorption on iron oxide doped MCM-41, Micropor Mesopor Mat., 2017, **245**, 8
2. B. Dou, C. Wang, Y. Song, H. Chen, B. Jiang, M. Yang, Y. Xu, Solid sorbents for in-situ CO_2 removal during sorption-enhanced steam reforming process: A review, Renew Sust Energ Rev., 2016, **53**, 536
3. M. Broda, C.R. Műller, Sol-gel derived, CaO-based, ZrO_2-stabilized CO_2 sorbent, Fuel, 2014,**127**, 94
4. M. S.Yancheshmeh, H. R. Radfarnia, M. C. Iliuta, High-temperature CO_2 sorbents and their application for hydrogen production by sorption enhanced steam reforming process, Chem. Eng. J., 2016, **283**, 420
5. L. Renuka, K.S. Anantharaju, S.C. Sharma, H.P. Nagaswarupa, S.C. Prashantha, H. Nagabhushana, Y.S. Vidya, Hollow microspheres Mg-doped ZrO_2 nanoparticles: Green assisted synthesis and applications in photocatalysis and photoluminescence, J Alloy Compd., 2016, **672**, 609
6. M.H. Oghaz, R.S. Razavi, M. Khajelakay, Optimizing sol-gel synthesis of magnesia-stabilized zirconia (MSZ) nanoparticles using Taguchi robust design for thermal barrier coatings (TBCs) applications, J. Sol-Gel Sci Technol., 2015, **73**, 227
7. I. Krivtsov, L. Faba, E. Díaz, S. Ordóñez, V. Avdin, S. Khainakov, J.R. Garcia, A new peroxo-route for the synthesis of Mg-Zr mixed oxides catalysts: Application in the gas phase acetone self-condensation, Appl Catal A-Gen., 2014, **477**, 26
8. X.Tian, Y. Zeng, T. Xiao, C. Yang, Y. Wang, S. Zhang, Fabrication and stabilization of nanocrystalline ordered mesoporous MgO-ZrO_2 solid solutions, Micropor Mesopor Mat., 2011,**143**, 357
9. J. Su, Y. Li, H. Wang, X. Yan, D. Pan, B. Fan, R. Li, Super-microporous solid base MgO-ZrO_2 composite and their application in biodiesel production, Chem Phys Lett., 2016, **663**, 61
10. F. Davar, N. Shayan, Preparation of zirconia-magnesia nanocomposite powders and coating by a sucrose mediated sol-gel method and investigation of its corrosion behavior, Ceram. Int., 2017, **43**, 3384
11. V. Nemec, H. Kaper, G. Pétaud, M. Ivanda, G. Štefanić, Impact of Mg^{+2} ion incorporation on the phase development of ZrO_2-type solid solutions and their application in the catalytic oxidation of carbon monixide, J. Mol. Struct., 2017, **1140**, 127
12. A. Mondal, S. Ram, Reconstructive phase formation of ZrO_2 nanoparticles in a new orthorhombic crystalstructure from an energized porous $ZrO(OH)_2 \cdot xH_2O$ precursor, Ceram. Int., 2004, **30**, 239
13. M. Stoia, P. Barvinschi, L. Barbu-Tudoran, A. Negrea, F. Barvinschi, Influence of thermal treatment on the formation of zirconia nanostructured powders by thermal decomposition of different precursors, J. Cryst. Growth, 2013, **381**, 93
14. N. Deb, An investigation on the solid –state thermal decomposition of bimetallic oxalate and tartrate coordination precursors of lanthanum (III) and palladium ions, J. Anal Appl. Pyrrolysis, 2008, **82**, 223
15. O. Gorban, S. Synyakina, G. Volkova, S. Gorban, T. Konstantiova, S. Lyubchik, Formation of metastable tetragonal zirconia nanoparticles: Competitive influence of the dopants and surface state, J. Solid State Chem., 2015, **232**, 249
16. L. C. Perera, O. Raymond, W. Henderson, P. J. Brothers, P. G. Plieger, Advances in beryllium coordination chemistry, Coord. Chem. Rev., 2017, **352**, 264
17. E. Bermejo, R. Carballo, A. Castiñeiras, A.B. Lago, Coordination of α-hydroxycarboxylic acids with first-row transition ions, Coordin Chem Rev., 2013, **257**, 2639
18. G. Peng, X. Wang, X. Chen, Y. Jiang, X. Mu, Zirconia-supported niobia catalyzed formation of propanol from 1,2-propanediol via dehydration and consecutive hydrogen transfer, J. Ind. Eng. Chem., 2014, **20**, 2641
19. L. Patron, O. Carp, I. Mindru, G. Marinescu, N. Stanica, I. Balint, Polynuclear coordination precursor compound for $M_3Fe_5O_{12}$ garnets (M=Y, Eu, Gd and Er). Part I. Synthesis of the precursors, J. Serb. Chem. Soc., 2005, **70(8-9)**, 1049
20. D. Gingasu, I. Mindru, L. Patron, G. Marinescu, S. Preda, J.M. Calderon-Moreno, N. Stanica, C. Andronescu, Nanocrystalline indium-based oxides by tartarate precursor route, Ceram. Int. 2014, **40**, 2267
21. S.E. Cabaniss, J.A. Leenheer, I.F. Mc Very, Aqueous infrared carboxylate absorbances: aliphatic di-acids, Spectrochim Acta A., 1998, **54**, 449
22. M.H. Al-Hazmi, Y.M. Choi, A.W. Apblett, Preparation of Zirconium Oxide Powder Using Zirconium Carboxylate Precursors, Advances in Physical Chemistry, 2014,**1**,1
23. S.M. Prabhu, S. Meenakshi, Novel one-pot synthesis of dicarboxylic acids mediated alginate-zirconium biopolymeric complex for defluoridation of water, Carbohyd Polym., 2015,**120**, 60
24. K. Nakamoto, Infrared and Raman spectra of Inorganic and Coordination Compounds, Part A: Theory and Applications in Inorganic Chemistry, John Wiley & Sons, 4th ed., 1986, p. 232
25. M. Nara, H. Morrii, M. Tanokura, Coordination to divalent cations by calcium-binding proteins studied by FTIR spectroscopy, Biochim. Biophys. Acta, 2013, **1828,** 2319
26. K. Mageshwari, S. S. Mali, R. Sathyamoorthy, P. S. Patil, Template-free synthesis of MgO nanoparticles for effective photocatalytic applications, Powder Technol., 2013, **249**, 456
27. P.B. Devaraja, D.N. Avadhani, S.C. Prashantha, H. Nagabhushana, S.C. Sharma, B.M. Nagabhushana, H.P. Nagaswarupa, Synthesis, structural and luminescence studies of magnesium oxide nanopowder, Spectrochim Acta A, 2014,**118**, 847
28. M. Răileanu, L. Todan, D. Crişan, N. Drăgan, M. Crişan, C. Stan, C. Andronescu, M. Voicescu, B.S. Vasile, A. Ianculescu, Sol-gel zirconia nanopowders with α-cyclodextrine as organic additive, J Alloy Compd., 2012, **517**,157
29. M.R. Gauna, M.S. Conconi, S. Gomez, G. Suárez, E.F. Aglietti, N.M. Rendtorff, Monoclinic-tetragonal zirconia quantification of commercial nanopowder mixtures by XRD and DTA, Ceram. Silik., 2015, **59(4)**, 318
30. Shen W,Tompsett GA, Hammond KD, Xing R, Dogan F, Grey CP, Conner Jr. WC, Auerbach SM, Huber GW. Liquid phase aldol condensation reactions with MgO–ZrO_2 and shape-selective nitrogen-substituted NaY. Appl. Catal. A: General, 2011, **392**, 57
31. I. Sádaba, M. Ojeda, R. Mariscal, J.L.G. Fierro, M. López Granados, Catalytic and structural properties of co-precipitated Mg-Zr mixed oxides for furfural valorization via aqueous aldol condensation with acetone, Appl. Catal. B., 2011,**101**, 638

****